applied sciences

IMPACT FACTOR 2.7

CITESCORE 4.5

Article

# Enhanced Osteoblast Adhesion and Proliferation on Vacuum Plasma-Treated Implant Surface

Hyun Jeong Jeon, Ara Jung, Hee Jin Kim, Jeong San Seo, Jun Young Kim, Moon Seop Yum, Bomi Gweon and Youbong Lim

Special Issue

Biomaterials and Bioimaging: From Biological Tissues to Biomedical Implants

Edited by

Dr. Bomi Gweon and Dr. Dohyung Lim

MDPI

https://doi.org/10.3390/app12199884

applied sciences

MDPI

*Article*

# Enhanced Osteoblast Adhesion and Proliferation on Vacuum Plasma-Treated Implant Surface

**Hyun Jeong Jeon [1,†], Ara Jung [2,3,†], Hee Jin Kim [2], Jeong San Seo [1], Jun Young Kim [1], Moon Seop Yum [4], Bomi Gweon [2,*] and Youbong Lim [1,*]**

1 Plasmapp Co., Ltd., Daejeon 18151, Korea
2 Department of Mechanical Engineering, Sejong University, Seoul 05006, Korea
3 Department of Biomedicine & Health Sciences, The Catholic University of Korea, Seoul 06591, Korea
4 Seoul Top Dental Clinic, 345 Omok-ro, Yangchun-gu, Seoul 07999, Korea
* Correspondence: bgweon@sejong.ac.kr (B.G.); ceo@plasmapp.com (Y.L.)
† These authors contributed equally to this work.

**Abstract:** In this study, we propose a vacuum plasma device for surface treatment of dental implants. This plasma device was designed to allow direct installation of sealed implant packaging containing the dental implant. In this manner, the dental implant could be treated with plasma under a moderate vacuum environment while remaining in a sterile condition. To assess the osseointegration efficiency, in vitro experiments using sandblasted, large grit, acid etching (SLA), calcium coated-SLA (CaSLA), and calcium coated-SLA with plasma treatment (PCaSLA) were performed. The implant surface was observed with scanning electron microscope (SEM) before and after plasma treatment. Thereafter, protein adsorption, cell adhesion, proliferation, and differentiation efficiency were investigated on the surface of each implant type using saos-2, an osteoblast. Plasma treatment significantly improved protein adsorption, cell adhesion, and cell proliferation efficiency compared to both CaSLA and SLA without damaging the calcium coating. According to the findings, the proposed vacuum plasma device has shown the potential to improve osseointegration efficiency. We believe that this plasma technology can be an innovative chairside solution that can be easily handled in the clinical field with superb usability.

**Keywords:** vacuum plasma-treated implant; plasma treatment; osseointegration; osteoblast adhesion; osteoblast proliferation; protein adsorption



**Citation:** Jeon, H.J.; Jung, A.; Kim, H.J.; Seo, J.S.; Kim, J.Y.; Yum, M.S.; Gweon, B.; Lim, Y. Enhanced Osteoblast Adhesion and Proliferation on Vacuum Plasma -Treated Implant Surface. *Appl. Sci.* **2022**, *12*, 9884. https://doi.org/10.3390/app12199884

Academic Editor: Giuliana Muzio

Received: 6 September 2022
Accepted: 28 September 2022
Published: 30 September 2022



## 1. Introduction

Dental implants made of titanium have become the most common technique for repairing extensive damage and loss of teeth. The clinical success of implants is dependent on a number of factors, including implant material, surface property, implant design, and bone quality of the patient [1]. Among these factors, implant material and surface property are the most critical determinants of in vivo reactivity, given that the implant is in direct contact with bone and induces osseointegration [1,2]. Commercially pure titanium (cpTi) is one of the most popular materials that are utilized in dental implants. cpTi has high corrosion resistance and releases a low level of metallic ions in bio-fluids; therefore, it is highly biocompatible [3–5]. In addition, given that titanium has high material strength, it is one of the best materials that can replace teeth which are usually exposed to compressive stress due to chewing activity. However, titanium is metal and not a bioactive substance by nature; therefore, a considerable period of time is required to achieve full integration between the titanium implant and the surrounding tissues [1,3,6].

To overcome this, various surface treatment methods have been developed, including the sandblasted, large grit, acid etching (SLA) technology [7–9]. The efficacy has been clinically validated and is now widely used worldwide. SLA is a technology that increases

the microroughness and hydrophilicity of a smooth titanium surface by spraying approximately 0.2 mm to 0.5 mm-diameter particles at high pressure and etching with an acidic solution [7]. The improved hydrophilicity of the implant surface increases the adsorption of extracellular matrix (ECM) protein. At the same time, the increased roughness of the surface allows the osteoblasts to adhere and grow into the curvature of the surfaces to form stable focal adhesions. Based on this, the SLA process can provide superior osteointegration of titanium implants [10]. Over time, however, various impurities will be deposited on the implant surface, decreasing surface energy and, eventually, deteriorating osteointegration efficiency [11–13]. In particular, hydrocarbon-based impurities are generally known to harm the adsorption of ECM and adhesion of osteoblast [12,13].

Therefore, researchers have put much effort into maintaining or restoring the bioactivity of the implant surface. For example, Straumann® developed an implant packaging technology that contains sodium chloride solution to prevent the implant surface from being contaminated by carbon in the ambient air and maintain a highly bioactive surface. The Ogawa group exposed the implant to a high-energy ultraviolet ray to remove hydrocarbon-based impurities and recover the hydrophilicity of the surface [11,12,14,15]. In addition, plasma treatment technologies were suggested to increase surface energy and reduce hydrocarbon impurities [16–18]. In particular, some recent studies have shown that plasma treatment creates a more hydrophilic surface and provides a better environment for cell adhesion and proliferation than UV-functionalization [19–21]. When plasma is discharged under atmospheric pressure or moderate vacuum condition, an incomplete ionization process produces high-energy radicals, which are extremely useful for the chemical modification of the material surfaces [22,23]. However, existing plasma devices for dental implants have extremely poor usability because implants must first be removed from their packaging, resulting in a break in the sterile barrier before being mounted and processed in the plasma device. Complexity and dysfunctional design of medical devices can indeed increase the risk of operator error and jeopardize patient safety [24,25]. Therefore, in order to more effectively apply plasma treatment technology to implants, usability needs to be dramatically improved.

This study suggested a vacuum plasma device that can uniformly treat the implant surface to improve osseointegration. The proposed device discharges plasma within the implant package without breaking the sterile barrier. Inside the implant package, a moderate vacuum, of approximately 5 Torr, was maintained, generating a uniform plasma across the entire surface of the dental implant. Several in vitro investigations were carried out employing SLA, calcium coated-SLA (CaSLA), and calcium coated-SLA with plasma treatment (PCaSLA) to assess the effect of plasma surface treatment and the osseointegration efficiency. Based on the outcomes of in vitro experiments, we confirmed that plasma treatment significantly improved protein adsorption and cell adhesion while maintaining the macro- and micro-roughness and calcium coating of the implant surfaces. In addition, plasma treatment was found to increase osteoblast proliferation and differentiation. Collectively, the proposed vacuum plasma treatment is believed to dramatically increase clinical outcomes in terms of osseointegration as well as usability.

## 2. Materials and Methods

### 2.1. Plasma Device

In order to treat the implant surface without opening the implant package and damaging the sterile barrier, we designed and developed a plasma generator (ACTILINK™, Plasmapp Co., Ltd., Daejeon, Korea) that operates in moderate vacuum conditions. As illustrated in Figure 1, a silicone block was positioned at the bottom of the package through which a needle could be inserted and used as a pumping outlet to create a vacuum inside the package. Gas inside the package was pumped out through this pumping outlet to maintain the implant package to approximately 5 Torr. In addition, to discharge plasma, our plasma device employed a dielectric barrier discharge (DBD) configuration. The packaging made of polyethylene (PE) served as a dielectric barrier, while the metal body of the device

enclosing the packaging served as a powered electrode. As the metal pumping outlet was connected to the ground, the implant within the package was grounded as well when the implant package was mounted on the device, and plasma was generated uniformly on the implant surface (Figure 1).

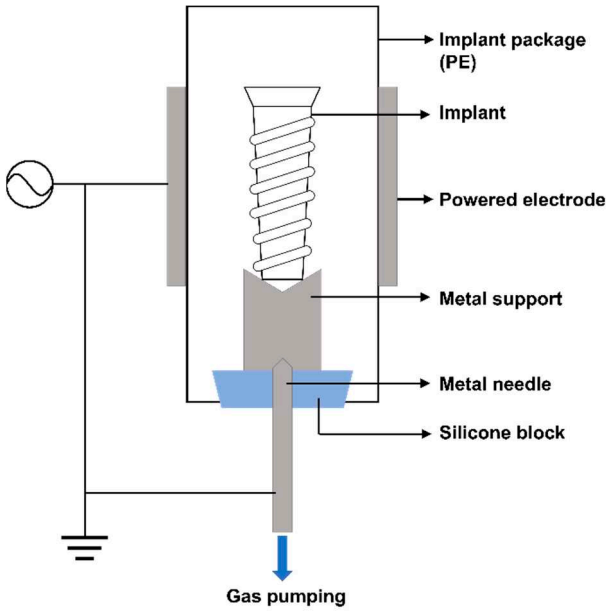


**Figure 1.** Schematic of the plasma generator (ACTILINK).

### *2.2. Implant Treatment Process*

S-L-A implants (SLA, #Anyone 4010, MEGEGEN) and calcium-coated S-L-A implants (CaSLA, #AnyOne IF4010, MEGAGEN) with a diameter of 4.0 mm and a length of 10 mm were prepared. We first demonstrated the effect of calcium coating by comparing SLA and CaSLA without plasma treatment. Given that both SLA and CaSLA implants were sterilized by gamma irradiation, there was no need to perform extra sterilization for in vitro experiments. To demonstrate the effect of plasma, CaSLA was compared with plasma-treated CaSLA (PCaSLA). As previously stated, the implant package was designed to fit in our plasma device, ACTILINK™, the implant package containing the implant was removed from the external medical blister package with Tyvek® lid and installed in ACTILINK™. Then, plasma was generated around the implant surface and maintained for 60 s at 5 Torr.

### *2.3. Hydrophilicity Test of Implant Surface*

Changes in the hydrophilicity of the implant surface by plasma treatment were confirmed by dipping the implants into the distilled water (DW). SLA, CaSLA, and PCaSLA were holed vertically, and the lower parts of the implants were slowly dipped into the DW reservoir. The degree of change in the hydrophilicity was evaluated by visually observing whether the DW rose along the thread of the implant.

### *2.4. Assessing Characteristics of Implant Surface Using SEM and EDS*

To confirm any physical deformation or chemical damage on the implant surface, the implant surface was imaged using a scanning electron microscope (SEM, Thermo Fisher Scientific, Phenom XL, Waltham, MA, USA) and Energy Dispersive X-ray Spectroscopy (EDS, Thermo Fisher Scientific, Phenom XL). Through SEM, image surface topography was analyzed, and, through EDS, the chemical composition in the implant surface was analyzed. In particular, we were interested in whether carbon content was reduced while calcium coating of CaSLA was intact after plasma treatment; therefore, we imaged the same CaSLA implant surface with SEM and EDS before and after plasma treatment to

compare the topographical and chemical changes caused by plasma treatment. To analyze the changes in the carbon and calcium contents, the weight contents ratio of carbon and calcium content was measured in five different samples by EDS. In addition, to determine the carbon reduction rate, the ratio between the amount of carbon reduction and the initial carbon content was measured for each sample.

### 2.5. Protein Adsorbtion Experiment

One of the representative extracellular matrices (ECMs) proteins, fibronectin, was utilized to investigate protein adsorption. Fibronectin (FN, Corning, New York, NY, USA, #356008, purity = 90%) was diluted in 1X phosphate buffer saline (PBS, GIBCO, #18912014) to a concentration of 50 μg/mL. FN solution of 200 μL volume was prepared in 96-well plates (SPL, Gyeongsan-si, Korea, #32096), and SLA, CaSLA, and PCaSLA were dipped separately into each well and left for 2 h. Then, to wash away non-adsorbed proteins from the implant surfaces, implants were gently shaken in 1X PBS, immersed in 2% 250 μL sodium dodecyl sulfate (SDS) solution (10% SDS solution, Biosesang, Gyeonggi-do, Korea, #SR2003-050-00), and stored at 37 °C for 18 h. After 18 h, proteins dissolved in this 2% SDS solution were quantified using a micro-BCA protein assay kit (Thermo Fisher Scientific, #23235). The quantification process was performed according to the protocol provided by the manufacturer. The optical density (O.D.) of the micro-BCA solution was determined using a microplate reader (Allsheng, Hangzhou, China, AMR-100) at 562 nm.

### 2.6. Quantification of Osteoblast Adhesion and Proliferation

To quantify cellular level responses, Saos-2, human osteoblast, was purchased (Korean Cell line bank, Seoul, Korea, #80023) and used. To stabilize cells, cells were sub-cultured at least three times after thawing. To prevent cells from adhering to the plate surfaces instead of the implant surfaces, cells were prepared in the non-treated plates (SPL, #32096). Cells were prepared in a dense suspension ($2.4 \times 10^6$ cells/well) and were placed into the 96-well plate right before the implants to be dipped into them, because the chance of cells adhering to the implant will become significantly lower once the cells settle down on the plate surface. After treating the implant surface with plasma, SLA, CaSLA, and PCaSLA were dipped into the cell suspension in an upright position and incubated at 37 °C for 2 h to allow cells to adhere to the implant surface. After 2 h of incubation, cell counting kit-8 (CCK-8, Dojindo, Kumamoto, Japan, #CK04) was used to quantify the cells adhering to the implant surface. The optical density (O.D.) of CCK-8 solution was determined using a microplate reader (Allsheng, AMR-100) at 450 nm. Cell proliferation was measured on days 3 and 7 of cell culture using the same procedure described above.

### 2.7. Quantification of Osteoblast Differentiation

Alkaline phosphatase (ALP) is one of the key enzymes that can be utilized as an indicator of osteoblast differentiation. Saos-2 cells were cultured on the implant surface using the same procedure described in Section 2.6. At day 7 of cell culture, implants with cells adhering on them were removed from the cell culture media and lysed in 500 μL of ALP assay buffer (Abcam, Cambridge, UK, #ab83369) and left for about 60 min on ice. After removing the implant, cell lysate was centrifuged at 4 °C at 13,000 rpm for 15 min, and the resulting supernatant was collected. An ALP assay kit (Abcam, #ab83369) was utilized to quantify ALP activity within the supernatant following the assay procedure provided by the manufacturer. The O.D. was measured at 405 nm by a microplate reader (Allsheng, AMR-100).

### 2.8. Staining and Imaging Cells on Implant Surface

To visualize cells adhered to the implant surfaces, cells were cultured following the same procedure described in Section 2.6. On 7 days of cell culture, implants were removed from the cell culture media, gently washed with 1X PBS, and placed in a formaldehyde solution (AMRESCO, Pittsburgh, PA, USA, #0493, Biotechnology grade) diluted to 3.7% in 1X PBS to fix cells. After that, cells were permeabilized in TritonX-100 solution (Bio

basic, Markham, ON, Canada, #TB0198, Biotech grade) diluted to 0.2% in 1X PBS for 10 min and washed three times with 1X PBS buffer. To visualize actin stress fiber, the implant on which fixed cells adhere was incubated in 1:50 Rhodamine phalloidin solution (Invitrogen, Waltham, MA, USA, #R415) and kept for 2 h. To image the cell nucleus, cells were then stained with 1:2000 Hoechst 33342 (Invitrogen, #H1399) solution for 5 min. In each step, cells were washed with 1X PBS three times. After finishing the staining process, the mounting solution (ProLong™ Glass Antifade Mountant, Invitrogen, #P36980) was dropped on the glass bottom confocal dish (SPL, #101350), and the implant was placed on top of the mounting solution. The cells on the implant surface were then imaged using an inverted fluorescence microscope (Leica DMi8) at 5× magnification.

### 2.9. Statistical Analysis

The sample size varied from 3 to 7 depending on the experiments. An unpaired *t*-test was performed to determine the statistical significance. Only the *p*-values lower than 0.05 were considered statistically significant. The symbols (*), (**), and (***) represent *p*-values < 0.05, <0.01, and <0.001, respectively.

## 3. Results

### 3.1. Hydrophilicity of Implant Surface before and after Plasma Treatment

As already reported in many previous studies, plasma treatment is known to increase the hydrophilicity of the surface. To confirm whether the plasma treatment successfully altered the wettability of the implant surface, the wetting characteristics of plasma-treated CaSLA (PCaSLA) were tested and compared to the one of SLA and CaSLA. Due to the calcium coating, the surface color of the implants shown in Figure 2B,C differs from that of the implants shown in Figure 2A. As shown in Figure 2, SLA and CaSLA implants repelled the surface of DW and were not wet at all. On the other hand, as soon as the lower part of the PCaSLA was immersed in DW, the DW rose rapidly along the thread, and the entire surface of PCaSLA was wetted in about 2 s. Therefore, we could confirm that plasma treatment transformed the hydrophobic feature of the CaSLA surface into a highly hydrophilic characteristic.

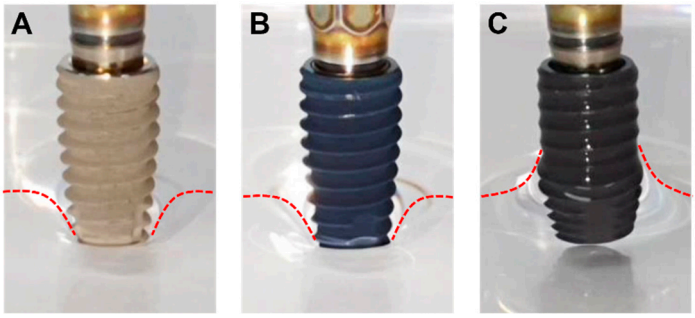


**Figure 2.** (**A**). SLA, (**B**). CaSLA, and (**C**). PCaSLA images after dipping the implants into a DW reservoir. Red dotted lines were drawn along the DW surfaces.

### 3.2. Surface Characteristics of Implant before and after Plasma Treatment

The microroughness created by SLA method is important for osteoblasts to adhere and grow on them. Therefore, when a CaSLA surface is treated with plasma, it is important not to harm this microroughness. In addition, as CaSLA was coated with calcium to assist the proliferation and differentiation of osteoblast, it is essential to confirm that plasma treatment does not damage the calcium layer coated on the CaSLA surface. Surface topography was observed through an SEM imaging surface, and atomic components of the surface were evaluated through EDS. We image the exact location of the implant surface before (CaSLA) and after the plasma treatment (PCaSLA). Comparing SEM images in Figure 3A,E revealed that the surface topography did not change following plasma treatment, and no physical damage was detected. Prior to the plasma treatment, large black dots, indicating carbon

impurities, were smeared on the implant surface (marked with a sharp sign (#) in Figure 3A). The EDS elemental map of carbon, shown in Figure 3D, confirmed that this black dot was a carbon impurity. Plasma treatment was demonstrated to reduce the area of this carbon impurity (Figure 3D,H), exposing the titanium surface that had been obscured by the carbon (indicated with an asterisk (*) in Figure 3F). The average reduction rate of carbon content following the plasma treatment was approximately 23.3% (Figure 3I). The graph shown in Figure 3I shows the carbon content measured in five different regions by EDS before (CaSLA) and after (PCaSLA) the plasma treatment. Although the difference between CaSLA and PCaSLA in Figure 3I was not statistically significant, a constant decrease in carbon content can be confirmed in Table 1 across all five samples.

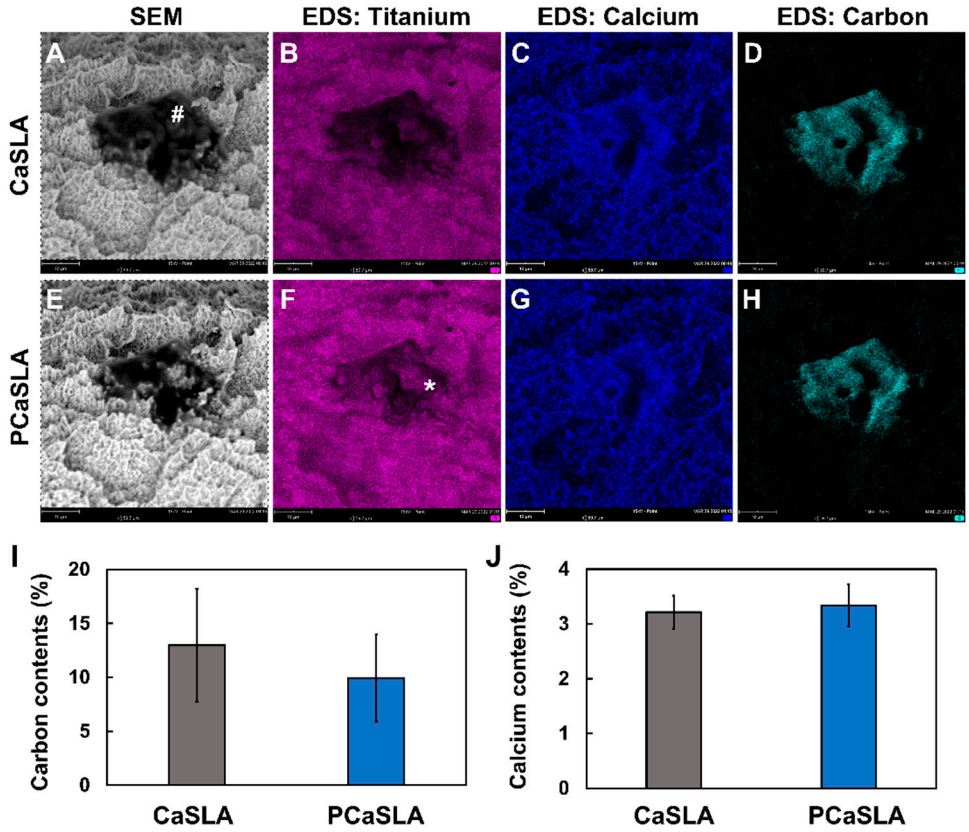


**Figure 3.** SEM and EDS images of CaSLA (**A**–**D**) and PCaSLA (**E**–**H**). (**I**). Carbon contents before (CaSLA) and after (PCaSLA) plasma treatment, and (**J**). calcium contents before (CaSLA) and after (PCaSLA). Carbon impurities present in the implant before plasma treatment (#). Titanium surface exposed after plasma treatment (*).

**Table 1.** Carbon reduction rate in each EDS analysis. Carbon reduction rate was assessed by comparing the carbon content measured by EDS prior to plasma treatment (CaSLA) and after plasma treatment (PaSLA).

| EDS Image Number | Carbon Reduction Rate (%) |
|---|---|
| #1 | 35.80886586 |
| #2 | 25.75539568 |
| #3 | 12.45318352 |
| #4 | 17.42268041 |
| #5 | 23.06220096 |

Unlike a decrease in carbon content, the plasma treatment has no effect on calcium coated on the titanium surface. As displayed in the EDS elemental map in Figure 3C,G, the overall distribution of calcium does not change by the plasma treatment. In addition,

according to the graph in Figure 3J, the calcium content of the implant surface before and after the plasma treatment was measured to be 3.2% and 3.3%, respectively, and the difference was not statistically significant. As such, it was also quantitatively confirmed that the calcium content of the implant surface was not affected by plasma.

### *3.3. Enhancement of Protein Adsorption by Plasma Treatment*

Once an implant is inserted into the body, ECM proteins in body fluid, such as fibrinogen, FN, and collagen, will be adsorbed to the implant surface, forming a primary adsorption layer. Then, cells will adhere to this layer to migrate and proliferate [26–28]. Therefore, protein adsorption efficiency is an important indicator that demonstrates the biocompatibility and the osseointegration efficiency of the implant. Among various ECM proteins, FN is known to contribute to forming focal adhesion of cells and assisting cell adhesion. Therefore, to compare the amount of protein adsorbed on different implant surfaces, SLA, CaSLA, and PCaSLA were prepared and immersed in fibronectin solution (50 μg/mL) for 2 h. The amount of protein adsorbed to the implant surfaces was quantified by micro-BCA assay kit, as shown in Figure 4A.

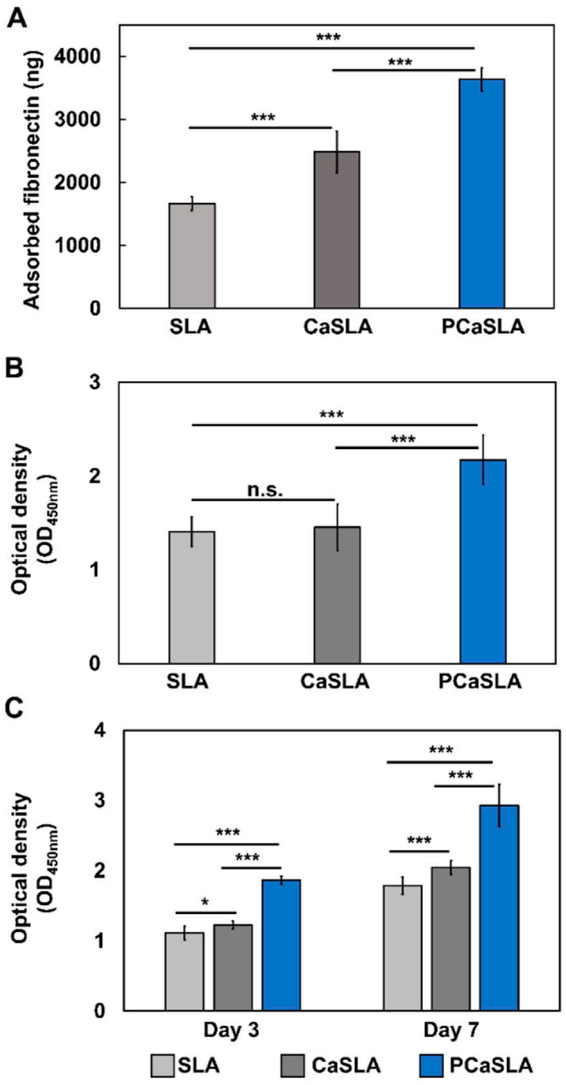


**Figure 4.** (**A**). the amount of adsorbed fibronectin, (**B**). the amount of adherent cells on SLA, CaSLA, and PCaSLA measured by CCK-8 assay after 2 h of culture, and (**C**). the amount of proliferated cells on SLA, CaSLA, and PCaSLA measured by CCK-8 assay at day 3 and day 7. [*, $p < 0.05$; ***, $p < 0.001$; n.s., not significant].

Figure 4A demonstrates that FN adsorption rate on CaSLA increased by 49.2% compared to the one on SLA. This result indicates that calcium coating on the SLA surface enhanced the protein adsorption efficiency. FN adsorption rate after plasma treatment (PCaSLA) improved the FN adsorption rate by 46.3% compared to the one on CaSLA. When SLA was coated with calcium and subsequently treated with plasma, it was shown to have much better protein adsorption efficiency than SLA without any treatment.

### 3.4. Improvement of Cell Adhesion and Proliferation by Plasma Treatment

Then, to evaluate the cell adhesion characteristics of three types of implants, osteoblasts were adhered to the implant surface by immersing the implants within the dense cell suspension. To investigate the initial adhesion of cells, the number of viable cells that adhered to the implant surface after incubation for 2 h was measured by determining the quantity of soluble formazan using CCK-8 assay. The number of cells on CaSLA did not differ considerably from that on SLA (Figure 4B). However, the number of cells on PCaSLA increased by 49.6% when compared to CaSLA, and 54.6% when compared to SLA (Figure 4B). Each experiment was carried out seven times, and the difference was shown to be statistically significant.

The number of cells was quantified after 3 and 7 days of incubation to further define the cell proliferation pattern. As shown in Figure 4C, the number of cells on CaSLA slightly increased by 9.9% on day 3 and by 14.2% on day 7 compared to SLA. The number of cells on plasma-treated CaSLA (PCaSLA) increased significantly by 52.4% and 43.4% on day 3 and 7, respectively, in comparison to the non-treated group (CaSLA). Furthermore, when compared to SLA, the number of cells on PCaSLA increased by 67.4% and 63.7% at day 3 and 7, respectively.

### 3.5. Distribution of Cells on Implant Surface

The distribution of cells on the implant surface was then observed by fluorescence imaging. After attaching cells to the implant surface, cells on the implant were incubated for the following seven days, fixed, and fluorescently labeled. To visualize the cell body and nucleus, cells were labeled with Phalloidin and Hoechst, respectively. When the cell suspensions were prepared, cells within the suspension would have slowly sunk to the bottom of the well plate due to their weight. Therefore, it was expected that cells would initially settle on the thread of the implant and then spread along the implant surface while proliferating. As predicted, the cells are predominantly spotted at the thread of the implant in all types of implants. As indicated by the arrowheads in Figure 5A, thick cell layers exist on top of the thread of SLA, CaSLA, and PCaSLA. However, cells on CaSLA have been demonstrated to be more spread out in the groove regions than cells on SLA (Figure 5A). Intriguingly, cells on PCaSLA were shown to be significantly more spread out than on CaSLA and SLA, with cells covering most of the surface, including the ridge regions (Figure 5A).

Then, the ALP activity was measured to determine the osteogenic differentiation efficiency. Given that it takes time for the cells to adhere to the implant surface, proliferate, and differentiate, ALP activity was measured on the seventh day of culture after attaching cells to the implants. In Figure 5B, it was shown that cells on CaSLA surface have a 14.7% improvement in ALP activity compared to that on SLA. In addition, PCaSLA seems to have enhanced ALP activity by 52.8% compared to CaSLA and 75.2% compared to SLA. As such, the ALP activity seems to improve with the calcium coating and plasma treatment.

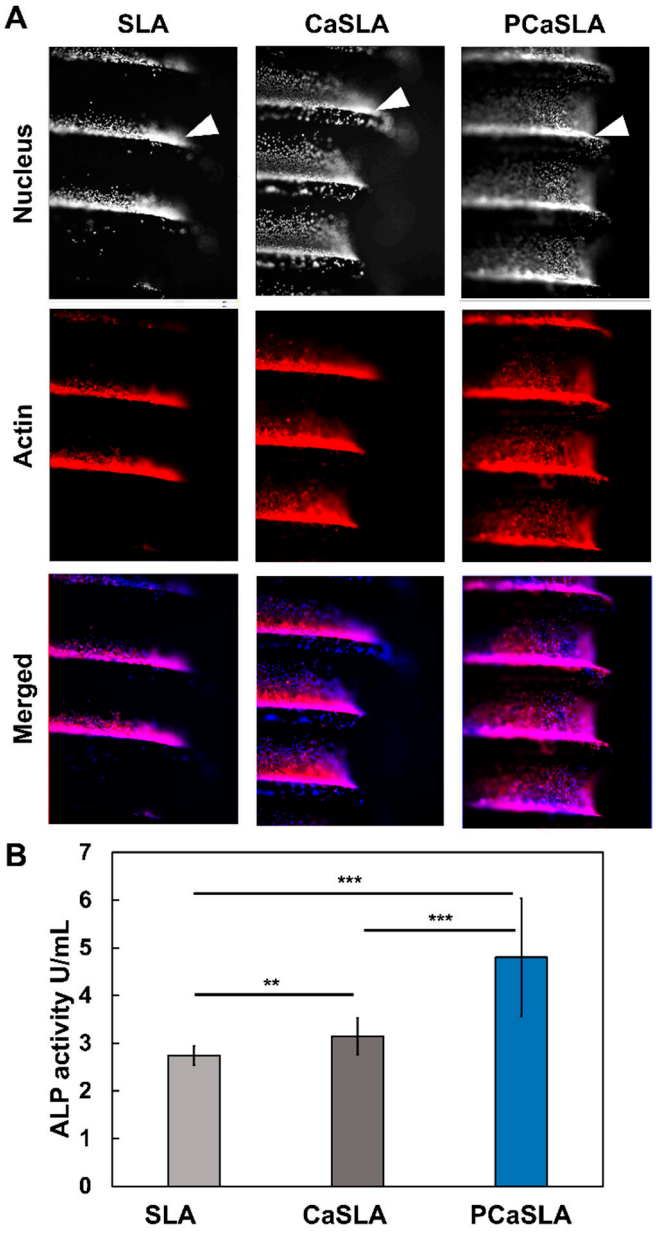


**Figure 5.** (**A**). Fluorescence images of cells labelled with Rhodamine phalloidin, and Hoechst 33,342 adhere on SLA, CaSLA, and PCaSLA surfaces (Nucleus images in the top row are shown in grey scale images. Actin images in the middle row are shown in red color. In the bottom row, the merged images show the nucleus in blue color and actin in red color. (**B**). ALP activity of cells on SLA, CaSLA, and PCaSLA at the 7th day of culture. [** $p < 0.01$, *** $p < 0.001$].

## 4. Discussion

UV-functionalization is a well-known method that improves bioactivity by changing the physicochemical properties of the implant surface [12,14,15,29]. Based on a large body of evidence indicating UV-functionalization can restore the bioactivity of the aged implant surfaces, UV irradiation devices have been developed as medical devices, capturing the attention of doctors in the dental field. For example, Therabeam® SuperOsseo, (Ushio Inc., Tokyo, Japan) and UV Activator (DIO implant Co. Ltd., Busan, Korea) are commercially available UV irradiation devices [30–32]. Previous studies on UV-functionalization have demonstrated that UV irradiation converts the implant surface to a hydrophilic property known to have a high affinity for protein and cells [15]. It has also been argued that UV irradiation excites the electrons from the valence band to the conduction band and

makes the implant surface, predominantly covered by $TiO_2$, positively charged [15,33]. Consequently, these hydrophilic and electrostatic properties have been shown to allow proteins and cells to attach directly to the implant surface, which in turn promotes osseointegration [12,14,15,29,33]. Plasma treatment, particularly air plasma treatment, is known to result in chemical effects similar to UV functionalization [34,35]. According to a previous study, $N_2$ plasma treatment on $TiO_2$ was shown to reduce $Ti^{4+}$ to $Ti^{3+}$ as in UV treatment, generating oxygen vacancies and leaving $TiO_2$ positively charged [34]. It has also been demonstrated that air-based $O_2$ plasma treatment forms a hydroxyl (OH) group on the $TiO_2$ surface, which is known to improve the hydrophilicity and binding affinity with proteins [35].

Based on these previous studies, the increase in hydrophilicity, improvement in protein adsorption, and cell adhesion observed in our study can be considered a result of the plasma-induced chemical process on the implant surface. In our in vitro investigation, the plasma-treated implant (PCaSLA) showed significantly higher levels of protein adsorption, osteoblast adhesion, and differentiation than the non-treated implant (CaSLA) (Figures 4 and 5). In addition, when observing the morphology of cells attached to PCaSLA, cells were more evenly and widely attached than that on CaSLA (Figure 5). These results are believed to be relevant to the increased hydrophilicity of the implant by the plasma (Figure 2). Ujino et al. have reported that plasma-induced surface modification increased hydrophilicity, cell adhesion, and further upregulated osteogenesis-related genes such as Runx2, ALP, and BMP-2 [36]. In addition, they observed twice as much calcium deposition on the plasma-treated titanium surface compared to the control, indicating a high degree of clinical relevance [36].

As mentioned in the Section 1, hydrocarbon-based impurities are generally known as detrimental to protein adsorption and osteoblast adhesion [12–14]. Aita et al. (2009) have shown a strong negative correlation between the level of carbon and the attractiveness of protein and cells. Accordingly, they suggested that carbon removal contributed to improving bone-implant integration [14]. Therefore, our experimental results in which plasma treatment reduced the amount of carbon on the implant surface are very encouraging (Figure 3). Plasma contains various high-energy species, including electrons, charged species, reactive oxygen species, metastable atoms, UV photons, etc. [37,38]. Given the fact that there is no extra gas supplied to our plasma device, the main discharge gas is air. In consequence, plasma will contain oxygen-related species such as $O^+$, $O^{2+}$, $O^-$, and $O^{3-}$ [23,39–41]. In a number of investigations related to plasma cleaning, researchers have demonstrated that carbon contaminants react with these oxygen-based species and become dissociated and reduced, releasing $CO_2$ and $H_2O$ [23,40,41]. Furthermore, continuous pumping to maintain a vacuum in the package removes these by-products immediately after they are released, eliminating the possibility of re-contamination.

More importantly, all of these plasma-bioactivation effects were achieved without causing any damage to the implant's existing calcium coating or microstructure. This is crucial in applying plasma treatment to the calcium-coated implant because if the plasma treatment damages the calcium coating, the osseointegration efficiency may be impaired rather than improved. According to many previous studies, calcium coating on the implant is known to promote osseointegration [42,43]. Feng et al. (2004) have demonstrated that calcium coating on the implant surface increases the adsorption of protein and improves the adhesion and proliferation of cells [42]. They reported that the calcium coating positively charged the implant surface with $Ca^{2+}$ ions, which created a favorable environment for FN and Vitronectin (VN) adsorption, leading in increased osteoblasts attachment [42]. This favorable effect of calcium coating was also seen in our results comparing SLA and CaSLA. Further, from such a benefit of calcium coating, we found that plasma treatment on the calcium-coated surface increased protein adsorption, cell adhesion, cell proliferation, and cell differentiation.

Collectively, the plasma treatment on the calcium-coated SLA surface bioactivates it by improving its hydrophilicity and removing carbon impurities. This plasma surface

modification resultingly improved FN protein adsorption, osteoblast adhesion, osteoblast proliferation, and osteogenic differentiation. We expect that these changes eventually can enhance osseointegration.

## 5. Conclusions

This research suggests a vacuum plasma device that provides uniform plasma treatment on the implant surface. SEM and EDS analysis confirmed that plasma treatment does not damage the microroughness and the calcium coating of the implant surface. In vitro experiments using osteoblast cells showed the possibility of promoting the osseointegration efficiency through plasma treatment. Moreover, by generating plasma within a sealed sterile package, the proposed plasma device markedly enhanced its usability so that the process could be easily carried out in clinical sites. Therefore, we anticipate that the vacuum plasma device developed in this work will be an innovative chairside solution applicable in the future to a variety of clinical fields.

**Author Contributions:** Conceptualization, J.Y.K., M.S.Y., B.G. and Y.L.; methodology, H.J.J., A.J., J.S.S., J.Y.K., M.S.Y., B.G. and Y.L.; investigation, H.J.J., A.J., H.J.K. and J.S.S.; resources, B.G. and Y.L.; writing—original draft preparation, H.J.J., A.J. and B.G.; writing—review and editing, B.G. and Y.L.; supervision, B.G. and Y.L.; funding acquisition, B.G. and Y.L. All authors have read and agreed to the published version of the manuscript.

**Funding:** This research was supported by the Technology development Program (S3142873) funded by the Ministry of SMEs and Startups (MSS, Korea) and by the National Research Foundation of Korea (NRF) grant funded by the Korea government (MSIT) (2022R1A2C2010940).

**Institutional Review Board Statement:** Not applicable.

**Informed Consent Statement:** Not applicable.

**Data Availability Statement:** The datasets generated and analyzed during the current research are available from the corresponding author on reasonable request.

**Acknowledgments:** We thank Kwang Bum Park for providing the implant fixtures and valuable advice.

**Conflicts of Interest:** H.J.J., J.S.S., J.Y.K., Y.L. are employees of Plasmapp Co., Ltd. B.G. received a research grant from Plasmapp Co., Ltd. The rest of the authors declare no conflict of interest related to this study.

## References

1. Aparicio, C.; Javier Gil, F.; Fonseca, C.; Barbosa, M.; Planell, J.A. Corrosion behaviour of commercially pure titanium shot blasted with different materials and sizes of shot particles for dental implant applications. *Biomaterials* **2003**, *24*, 263–273. [CrossRef]
2. Sanchez-Perez, A.; Nicolas-Silvente, A.I.; Sanchez-Matas, C.; Muñoz-Guzon, F.; Navarro-Cuellar, C.; Romanos, G.E. Influence on Bone-to-Implant Contact of Non-Thermal Low-Pressure Argon Plasma: An Experimental Study in Rats. *Appl. Sci.* **2020**, *10*, 3069. [CrossRef]
3. Schuler, M.; Trentin, D.; Textor, M.; Tosatti, S.G. Biomedical interfaces: Titanium surface technology for implants and cell carriers. *Nanomedicine* **2006**, *1*, 449–463. [CrossRef]
4. Textor, M.; Sittig, C.; Frauchiger, V.; Tosatti, S.; Brunette, D.M. Properties and Biological Significance of Natural Oxide Films on Titanium and Its Alloys. In *Titanium in Medicine: Material Science, Surface Science, Engineering, Biological Responses and Medical Applications*; Brunette, D.M., Tengvall, P., Textor, M., Thomsen, P., Eds.; Springer: Berlin/Heidelberg, Germany, 2001; pp. 171–230. [CrossRef]
5. Jansen, J.A.; Vonrecum, A.F.; Vanderwaerden, J.P.C.M.; Degroot, K. Soft-Tissue Response to Different Types of Sintered Metal Fiber-Web Materials. *Biomaterials* **1992**, *13*, 959–968. [CrossRef]
6. McCracken, M. Dental Implant Materials: Commercially Pure Titanium and Titanium Alloys. *J. Prosthodont.* **1999**, *8*, 40–43. [CrossRef] [PubMed]
7. Verardi, S.; Swoboda, J.; Rebaudi, F.; Rebaudi, A. Osteointegration of Tissue-Level Implants with Very Low Insertion Torque in Soft Bone: A Clinical Study on SLA Surface Treatment. *Implant Dent.* **2018**, *27*, 5–9. [CrossRef]
8. Gianfreda, F.; Raffone, C.; Antonacci, D.; Mussano, F.; Genova, T.; Chinigò, G.; Canullo, L.; Bollero, P. Early Biological Response of an Ultra-Hydrophilic Implant Surface Activated by Salts and Dry Technology: An In-Vitro Study. *Appl. Sci.* **2021**, *11*, 6120. [CrossRef]

9. Hou, P.-J.; Syam, S.; Lan, W.-C.; Ou, K.-L.; Huang, B.-H.; Chan, K.-C.; Tsai, C.-H.; Saito, T.; Liu, C.-M.; Chou, H.-H.; et al. Development of a Surface-Functionalized Titanium Implant for Promoting Osseointegration: Surface Characteristics, Hemocompatibility, and In Vivo Evaluation. *Appl. Sci.* **2020**, *10*, 8582. [CrossRef]
10. Zuanazzi, D.; Xiao, Y.; Siqueira, W.L. Evaluating protein binding specificity of titanium surfaces through mass spectrometry–based proteomics. *Clin. Oral Investig.* **2021**, *25*, 2281–2296. [CrossRef]
11. de Avila, E.; Lima, B.; Sekiya, T.; Torii, Y.; Ogawa, T.; Shi, W.; Lux, R. Effect of UV-photofunctionalization on oral bacterial attachment and biofilm formation to titanium implant material. *Biomaterials* **2015**, *67*, 84–92. [CrossRef]
12. Att, W.; Hori, N.; Iwasa, F.; Yamada, M.; Ueno, T.; Ogawa, T. The effect of UV-photofunctionalization on the time-related bioactivity of titanium and chromium–cobalt alloys. *Biomaterials* **2009**, *30*, 4268–4276. [CrossRef] [PubMed]
13. Kilpadi, D.V.; E Lemons, J.; Liu, J.; Raikar, G.N.; Weimer, J.J.; Vohra, Y. Cleaning and heat-treatment effects on unalloyed titanium implant surfaces. *Int. J. Oral Maxillofac. Implants* **2000**, *15*, 219–230. [PubMed]
14. Aita, H.; Hori, N.; Takeuchi, M.; Suzuki, T.; Yamada, M.; Anpo, M.; Ogawa, T. The effect of ultraviolet functionalization of titanium on integration with bone. *Biomaterials* **2009**, *30*, 1015–1025. [CrossRef]
15. Iwasa, F.; Hori, N.; Ueno, T.; Minamikawa, H.; Yamada, M.; Ogawa, T. Enhancement of osteoblast adhesion to UV-photofunctionalized titanium via an electrostatic mechanism. *Biomaterials* **2010**, *31*, 2717–2727. [CrossRef]
16. Danna, N.R.; Beutel, B.G.; Tovar, N.; Witek, L.; Marin, C.; Bonfante, E.A.; Granato, R.; Suzuki, M.; Coelho, P.G. Assessment of Atmospheric Pressure Plasma Treatment for Implant Osseointegration. *BioMed Res. Int.* **2015**, *2015*, 761718. [CrossRef] [PubMed]
17. Guastaldi, F.P.S.; Yoo, D.; Marin, C.; Jimbo, R.; Tovar, N.; Zanetta-Barbosa, D.; Coelho, P.G. Plasma Treatment Maintains Surface Energy of the Implant Surface and Enhances Osseointegration. *Int. J. Biomater.* **2013**, *2013*, 354125. [CrossRef] [PubMed]
18. Hui, W.L.; Perrotti, V.; Iaculli, F.; Piattelli, A.; Quaranta, A. The Emerging Role of Cold Atmospheric Plasma in Implantology: A Review of the Literature. *Nanomaterials* **2020**, *10*, 1505. [CrossRef] [PubMed]
19. Henningsen, A.; Smeets, R.; Heuberger, R.; Jung, O.T.; Hanken, H.; Heiland, M.; Cacaci, C.; Precht, C. Changes in surface characteristics of titanium and zirconia after surface treatment with ultraviolet light or non-thermal plasma. *Eur. J. Oral Sci.* **2018**, *126*, 126–134. [CrossRef]
20. Yang, Y.; Zheng, M.; Liao, Y.; Zhou, J.; Li, H.; Tan, J. Different behavior of human gingival fibroblasts on surface modified zirconia: A comparison between ultraviolet (UV) light and plasma. *Dent. Mater. J.* **2019**, *38*, 756–763. [CrossRef] [PubMed]
21. Matsumoto, T.; Tashiro, Y.; Komasa, S.; Miyake, A.; Komasa, Y.; Okazaki, J. Effects of Surface Modification on Adsorption Behavior of Cell and Protein on Titanium Surface by Using Quartz Crystal Microbalance System. *Materials* **2021**, *14*, 97. [CrossRef] [PubMed]
22. Banerjee, K.; Kumar, S.; Bremmell, K.; Griesser, H. Molecular-level removal of proteinaceous contamination from model surfaces and biomedical device materials by air plasma treatment. *J. Hosp. Infect.* **2010**, *76*, 234–242. [CrossRef]
23. Gong, X.; Lin, Y.; Li, X.; Wu, A.; Zhang, H.; Yan, J.; Du, C. Decomposition of volatile organic compounds using gliding arc discharge plasma. *J. Air Waste Manag. Assoc.* **2020**, *70*, 138–157. [CrossRef] [PubMed]
24. Gruchmann, T. The impact of usability on patient safety. *Biomed. Insa. Technol.* **2005**, *39*, 462–465.
25. Zhang, J.; Johnson, T.; Patel, V.L.; Paige, D.L.; Kubose, T. Using usability heuristics to evaluate patient safety of medical devices. *J. Biomed. Inform.* **2003**, *36*, 23–30. [CrossRef]
26. Cai, S.; Wu, C.; Yang, W.; Liang, W.; Yu, H.; Liu, L. Recent advance in surface modification for regulating cell adhesion and behaviors. *Nanotechnol. Rev.* **2020**, *9*, 971–989. [CrossRef]
27. Guo, S.; Zhu, X.; Li, M.; Shi, L.; Ong, J.L.T.; Jańczewski, D.; Neoh, K.G. Parallel Control over Surface Charge and Wettability Using Polyelectrolyte Architecture: Effect on Protein Adsorption and Cell Adhesion. *ACS Appl. Mater. Interfaces* **2016**, *8*, 30552–30563. [CrossRef]
28. Ayala, R.; Zhang, C.; Yang, D.; Hwang, Y.; Aung, A.; Shroff, S.S.; Arce, F.T.; Lal, R.; Arya, G.; Varghese, S. Engineering the cell-material interface for controlling stem cell adhesion, migration, and differentiation. *Biomaterials* **2011**, *32*, 3700–3711. [CrossRef] [PubMed]
29. Ogawa, T. Ultraviolet Photofunctionalization of Titanium Implants. *Int. J. Oral Maxillofac. Implants* **2014**, *29*, e95–e102. [CrossRef]
30. Razali, M.; Ngeow, W.C.; Omar, R.A.; Chai, W.L. An Integrated Overview of Ultraviolet Technology for Reversing Titanium Dental Implant Degradation: Mechanism of Reaction and Effectivity. *Appl. Sci.* **2020**, *10*, 1654. [CrossRef]
31. Soltanzadeh, P.; Ghassemi, A.; Ishijima, M.; Tanaka, M.; Park, W.; Iwasaki, C.; Hirota, M.; Ogawa, T. Success rate and strength of osseointegration of immediately loaded UV-photofunctionalized implants in a rat model. *J. Prosthet. Dent.* **2017**, *118*, 357–362. [CrossRef]
32. Kim, H.S.; Lee, J.I.; Yang, S.S.; Kim, B.S.; Kim, B.C.; Lee, J. The effect of alendronate soaking and ultraviolet treatment on bone-implant interface. *Clin. Oral Implants Res.* **2017**, *28*, 1164–1172. [CrossRef] [PubMed]
33. Wang, R.; Hashimoto, K.; Fujishima, A.; Chikuni, M.; Kojima, E.; Kitamura, A.; Shimohigoshi, M.; Watanabe, T. Light-induced amphiphilic surfaces. *Nature* **1997**, *388*, 431–432. [CrossRef]
34. Liu, X.; Hua, R.; Niu, J.; Zhang, Z.; Zhang, J. N2 plasma treatment TiO2 nanosheets for enhanced visible light-driven photocatalysis. *J. Alloys Compd.* **2021**, *881*, 160509. [CrossRef]
35. Kim, W.J.; Kim, S.; Lee, B.S.; Kim, A.; Ah, C.S.; Huh, C.; Sung, G.Y.; Yun, W.S. Enhanced protein immobilization effi-ciency on a TiO2 surface modified with a hydroxyl functional group. *Langmuir* **2009**, *25*, 11692–11697. [CrossRef] [PubMed]

36. Ujino, D.; Nishizaki, H.; Higuchi, S.; Komasa, S.; Okazaki, J. Effect of plasma treatment of titanium surface on biocom-patibility. *Appl. Sci.* **2019**, *9*, 2257. [CrossRef]
37. Volkov, A.G.; Xu, K.G.; Kolobov, V.I. Plasma-generated reactive oxygen and nitrogen species can lead to closure, locking and constriction of the Dionaea muscipula Ellis trap. *J. R. Soc. Interface* **2019**, *16*, 20180713. [CrossRef]
38. Nastuta, A.V.; Gerling, T. Cold Atmospheric Pressure Plasma Jet Operated in Ar and He: From Basic Plasma Properties to Vacuum Ultraviolet, Electric Field and Safety Thresholds Measurements in Plasma Medicine. *Appl. Sci.* **2022**, *12*, 644. [CrossRef]
39. Dukes, C.A.; Baragiola, R.A. Compact plasma source for removal of hydrocarbons for surface analysis. *Surf. Interface Anal.* **2010**, *42*, 40–44. [CrossRef]
40. Sasmazel, H.T.; Alazzawi, M.; Alsahib, N.K.A. Atmospheric Pressure Plasma Surface Treatment of Polymers and Influence on Cell Cultivation. *Molecules* **2021**, *26*, 1665. [CrossRef] [PubMed]
41. Graves, D.B. Reactive Species from Cold Atmospheric Plasma: Implications for Cancer Therapy. *Plasma Process. Polym.* **2014**, *11*, 1120–1127. [CrossRef]
42. Feng, B.; Weng, J.; Yang, B.; Qu, S.; Zhang, X. Characterization of titanium surfaces with calcium and phosphate and osteoblast adhesion. *Biomaterials* **2004**, *25*, 3421–3428. [CrossRef]
43. Park, J.W.; Kim, H.K.; Kim, Y.J.; An, C.H.; Hanawa, T. Enhanced osteoconductivity of micro-structured titanium implants (XiVE S CELLplus((TM))) by addition of surface calcium chemistry: A histomorphometric study in the rabbit femur. *Clin. Oral Implants Res.* **2009**, *20*, 684–690. [CrossRef] [PubMed]